Modeling Ultrafiltration of Complex Biological Solutions

E. Darnon, M. P. Belleville, and G. M. Rios
Institut Europeen des Membranes, CC047, UM2, 34095 Montpellier cedex 5, France

The ultrafiltration of a single protein (β-lactoglobulin) solution was compared with a mixture of yeast extract and β-lactoglobulin to show that, even when all the compounds of a complex biological solution interfere with the results of filtration, it can estimate its performance just using some major assumptions connected to a mass-transfer model. Preliminary experiments based on these assumptions showed that the filtration of a single rejected protein like β-lactoglobulin builds a dynamic layer at the wall, the selectivity and resistance of control by the protein concentration and formation of this dynamic membrane. Adding yeast extract, a complex biological medium, can alter this layer. But at neutral pH, away from the protein isoelectric point, these modifications are weak and their effects more negligible than those arising from a modified concentration. Using these assumptions, a model based on the theory of thermodynamics of irreversible processes is proposed that provides the correct description of selectivity and flux during the filtration of such complex and badly known mixtures.

Introduction

A large number of important commercial membrane processes involve the filtration of biological solutions containing proteins, peptides, amino acids, salts, and other compounds, such as organic acids, sugars, and vitamins; for example, the concentration of whey proteins in the production of a variety of dairy products, the filtration of wine, and the purification units in downstream processing. Although ultrafiltration (UF) is already extensively used, there is currently little understanding and model specifically developed for such complex systems. Several mechanisms may be involved in the transfer of a particular solute through UF membranes. The first one is steric hindrance: the membrane is considered a sieving barrier that retains molecules according to their size. Besides this notion, it is also worth considering van der Waals, electrostatic or chemical interactions between membrane and solutes or even among solutes themselves; they play a large part in the building of filtration selectivity. The total resulting effects are complex. A typical case is biological solutions, where all these interactions are involved on numerous and often poorly understood solutes.

A number of studies have demonstrated that protein fouling is one of the critical factors determining the filtrate flux during UF processes. Marshall et al. (1993) reviewed these studies and the role of the different operating conditions. More recently, some authors proposed models to describe the transmission of solutes (Rabiller-Baudry et al., 2000) and the flux (Palecek and Zydney, 1994), starting from the known properties of membranes and solutes (surface potential, charge density, and the electrophoretic mobility of solutes). Another way to describe transport is the phenomenological approach. Nakao and Kimura (1981) characterized the fouling layer formed during tangential filtration—the so-called dynamic membrane—with a model based on the thermodynamics of irreversible processes. In this approach, the membrane and the dynamic layer are considered as a black box. The "pore model," first established by Verniory et al. (1973) and further modified (see Nakao, 1994; Zhao et al., 2000), brings complementary information on the "membrane + deposit" system. It is used to characterize rp, the pore radius, and $Ak/\Delta x$, the ratio of Ak, the total pore to the effective membrane area, to Δx, the membrane thickness, assuming cylindrical uniform pores and spherical solutes.

Most of the published studies on transport modeling deal with known proteins or known mixtures of proteins and buffer (Nakao and Kimura, 1981; Bullon et al., 2000). On the contrary, industrial processes apply to poorly known solutions that are much more complex than those treated in theoretical

Correspondence concerning this article should be addressed to E. Darnon.

studies. Based on Nakao's approach and specific assumptions, our aim is, thus, to propose a new way to depict solute and water transfer through UF membranes when the feed solution is complex and mostly undetermined (because of the difficulties in identifying the solutes and in obtaining their characteristics: size, density of charge, etc.). Feed solutions chosen in this study are, thus, very complex and not entirely determined as a real solution would be. Two components have been chosen to represent different classes of compounds: β-lactoglobulin, as a model for the large proteins completely rejected by the membrane, and yeast extract (that contains peptides, amino acids, and salts) to represent the complex part of the solution. To quantify the performance of the separation and to analyze fouling and selectivity during filtration, two criteria (permeate flux and transmission rate of a reference molecule added to the mixture as a tracer) have been chosen. Both components were filtered separately under various operating conditions (concentration and ionic strength) to point out the relative importance of each one as regards to filtration results. From Nakao's approach, the pore size and porosity of the "membrane + deposit" system as a function of operating conditions follow. Then, the filtration of mixtures has been carried out and their results compared to single-compound filtration. As presented in this article, this comparison gives a way to extend Nakao's approach to complex mixture analysis by an original procedure.

Theoretical Background

Solute rejection by UF membrane leads to the formation of a deposit, often referred to as dynamic membrane, that is composed of all the species deposited at the wall (irreversible or reversible process). Next to the dynamic membrane, the concentration polarization phenomenon occurs in the module and is responsible for a concentration gradient in the solution, between the bulk and the membrane. Using the description of these two phenomena (Figure 1), the real characteristics of the membrane at work can be taken from the experimental results provided by the filtration of a well-known and size-determined reference solute. More details are given in the following paragraphs.

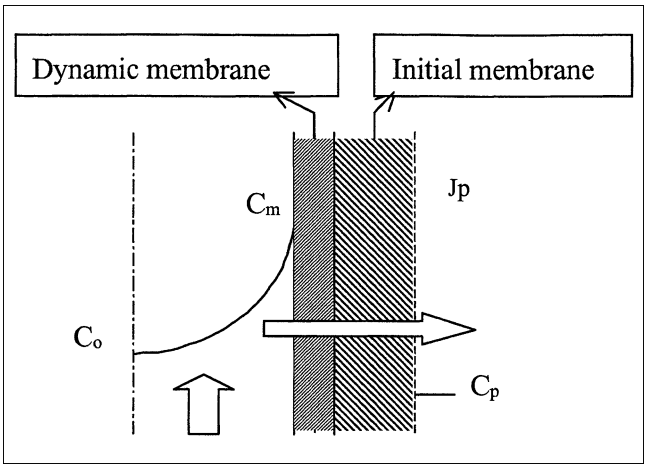

Figure 1. Concentration polarization and dynamic membrane formation.

The film model is used to describe the polarization in the boundary layer. Equation 1 results from the mass balance, which accounts for the convective flow that brings the solute from the bulk to the membrane, and the diffusive flow that settles in the opposite direction due to the concentration gradient

$$JpC_p = JpC + D\frac{dC}{dy} \tag{1}$$

with Jp the permeate or solvent flux ($m^3 \cdot m^{-2} \cdot s^{-1}$), C the solute concentration ($kg \cdot m^{-3}$) in the layer, C_p the solute concentration in the permeate ($kg \cdot m^{-3}$), and D the solute diffusivity ($m^2 \cdot s^{-1}$). Assuming that D is constant, the integration of this relationship in the boundary layer between $y = 0$ at the wall ($C = C_m$) and $y = \delta$, the boundary-layer thickness ($C = C_o$)] gives

$$Jp = \frac{D}{\delta} \ln\left(\frac{C_m - C_p}{C_o - C_p}\right) \tag{2}$$

The ratio D/δ is the diffusive mass-transfer coefficient, also written k ($m \cdot s^{-1}$). This coefficient can be estimated with correlations that put together the three classic dimensionless numbers Re ($\rho ud/\mu$), Sc ($\mu/\rho D$), Sh (dk/D) (van den Berg et al., 1989). In the area of operating conditions (Re greater than 5,000, turbulent flow, and Sc greater than 1,000 for the filtered solutes), van den Berg et al. suggest that the Harriot–Hamilton correlation be used, as expressed in Eq. 3

$$Sh = 0.0096 Re^{0.91} Sc^{0.35} \tag{3}$$

Starting from the bulk concentration (C_o) and the measurable results of filtration (Jp, C_p), it becomes possible with k to estimate the concentration of a given solute at the wall (C_m).

As said before, the solute transfer through the membrane, which means from C_m to C_p, can be described using the phenomenological approach. The various flux (solutes and water) through the black box associated with the membrane + deposit system are assumed to be linear functions of their origin (applied forces). The transport equations can be written as

$$Jp = Lp(\Delta P - \sigma \Delta \pi) \tag{4}$$

$$Js = P\Delta C_s + (1 - \sigma)\overline{C}_s Jp \tag{5}$$

where Js is the solute flux ($kg \cdot m^{-2} \cdot s^{-1}$); ΔP is the transmembrane pressure, which constitutes the process driving force, and $\Delta \pi$ is the osmotic pressure difference, a consequence of solute discrimination at the membrane walls (both expressed in Pa). In these equations, the membrane characteristics are described through three parameters: Lp, the pure water permeability ($m \cdot s^{-1} \cdot Pa^{-1}$); P, the solute permeability ($m \cdot s^{-1}$); and σ, the reflection coefficient in the 0 (no retention of the solute) to 1 (completely rejected solute) range. Also, ΔC_s is the difference between the concentrations of the solute at the inner (C_m) and outer (C_p) membrane walls, and $\overline{C_s}$ is the average concentration inside the black box. In those cases where ΔC_s is reduced, a simple use of the logarithmic

mean gives the proper estimation of $\overline{C_s}$. Otherwise, Nakao suggests preferentially the following equations

$$R_r = 1 - Tr_r = \sigma \frac{(1-F)}{1-\sigma F} \tag{6}$$

$$F = \exp\left(-\frac{(1-\sigma)Jp}{P}\right) \tag{7}$$

where Tr_r is the intrinsic transmission rate (also called intrinsic sieving coefficient), defined as the ratio between C_p and C_m, and R_r is the retention rate.

A clear distinction must to be made between this intrinsic transmission rate, Tr_r, the observed transmission rate (Tr_o, the ratio between C_p and C_o), and the reflection coefficient σ. Indeed, $(1-\sigma)$ is the transmission limit obtained at very high convective flow, while Tr_r is the pure separation factor due to the black box considering that there is no concentration polarization, and Tr_o is the observed transmission that accounts for polarization limitation and represents the effective process selectivity as given by experiments.

Most of the time, Lp is determined from the water permeate flux as measured on the prefouled membrane (that means when $C_m = 0$). However, this method is incorrect in the presence of a reversible deposit. For this reason, we have chosen to estimate Lp, considering that for a completely rejected solute σ is close to 1. Equation 8 follows

$$Jp = Lp(\Delta P - \pi_m) \tag{8}$$

There are different ways of accounting for the osmotic pressure at the wall on the retentate side (π_m). More often, an expression derived from the virial theory is chosen and gives the osmotic pressure as a function of the concentration with a polynomial expression of degree 3 (van den Berg et al., 1989; Prabhakar et al., 2000) or 2 (van Reis et al., 1997). As these correlations are not always clearly established, some authors use the van't Hoff law that gives a good estimation (Niemi and Palosaari, 1993)

$$\pi_m = C_m RgT/M \tag{9}$$

where Rg is the gas constant ($8.314 \times \mathrm{J \cdot mol^{-1} \cdot K^{-1}}$), M is the molecular weight ($\mathrm{kg \cdot mol^{-1}}$), and T is the temperature (K). The permeate flux relation becomes

$$Jp = Lp(\Delta P - C_m RgT/M) \tag{10}$$

This relationship, valuable for completely rejected solutes like β-lactoglobulin, must be modified when solutes are not completely rejected by the membrane. In that case, the osmotic contribution (which is $\Delta\pi$ rather than π_m) is multiplied by σ. When a mixture is filtered, the total osmotic contribution is obtained by adding the osmotic contribution of each solute.

The phenomenological coefficients (σ, P) are estimated at the minimum standard deviation between direct calculations of Tr_r and experimental values derived from the film theory. More precisely, the final (σ, P) are obtained at the minimum of the sum of the square of the difference between Tr_r calculated from the TIP model (Eq. 6), and Tr_r deduced from the film model (Eq. 2) and experimental results.

As was said in the Introduction, the pore theory is then used to convert these phenomenological coefficients, obtained with a given solute, into intrinsic characteristics of the black-box system. In this model, the solute flux is expressed as the combination of a convective and a diffusive flow

$$Js = D_o f(\lambda) S_D(\lambda) \frac{Ak}{\Delta x} \Delta C_s + Jp \overline{C}_s g(\lambda) S_F(\lambda) \tag{11}$$

where $f(\lambda)$ and $g(\lambda)$ are two correction factors that account for the wall effects, while S_F and S_D are steric factors deduced from Ferry and Zeman studies. Nakao (1994) and Zhao et al. (2000) report the following relationships between λ, the solute to pore-size ratio, and S_D, S_F, f, g, respectively

$$S_D = (1-\lambda)^2 \tag{12}$$

$$S_F = 2(1-\lambda)^2 - (1-\lambda)^4 \tag{13}$$

$$f(\lambda) = \frac{1 - 2.1\lambda + 2.1\lambda^3 - 1.7\lambda^5 + 0.73\lambda^6}{1 - 0.76\lambda^5} \tag{14}$$

$$g(\lambda) = \frac{1 - 0.66\lambda^2 - 0.2\lambda^5}{1 - 0.76\lambda^5} \tag{15}$$

The TIP and pore theory models are linked through the permeate flux equation, and the phenomenological parameters can be expressed as a function of the characteristics

$$\sigma = 1 - g(\lambda) S_F \tag{16}$$

$$P = D f(\lambda) S_D \frac{Ak}{\Delta x} \tag{17}$$

$$Lp = \frac{rp^2}{8\mu} \frac{Ak}{\Delta x} \tag{18}$$

This last equation (Poiseuille law) directly connects the rp and $Ak/\Delta x$ characteristics. Consequently, their calculation may be realized simultaneously with σ and P estimations.

This entire estimation method has already been applied to the filtration of one single solute solution (in the presence of a reference molecule) to characterize the fouled membrane (Nakao and Kimura, 1981; Sarrade et al., 1994; Bullon et al., 2000). On the other hand, we can imagine finding the permeate flux and transmission rate of a particular solute on a given membrane when its characteristics are known. A part of our work aims at validating this original procedure.

Experimental Studies

Solutions

Species involved in this study are: yeast extract (YE) (Biokar Diagnostic, France), β-lactoglobulin (beta) (Protarmor 865, Armor proteins), vitamin B12 (B12; our reference molecule), and sodium chloride (Merck). The known characteristics of these components are shown in Table 1.

Yeast extract was analyzed by size exclusion-HPLC using a TSK2500PW column; detection was made at 215 and 280 nm. With this method, the effective mass distribution of proteins and peptides was found between 100 and 5,000 Da.

Table 1. Characteristics of β-Lactoglobulin, Yeast Extract, and Vitamin B12

Species	Characteristics
β-lactoglobulin (beta)	Globular protein MW dimer : 36 kD, rs^* = 2.7 nm (dimer forms at neutral pH) IEP = 5.3
Yeast extract (YE): 1/Protein and assimilated† 2/Salts 3/Other contents:	MW: 100–5000 D** Mass fraction: 75% Mass fraction: 15% Mass fraction: 10%
Vitamin B12 (B12)	MW: 1.35 kD, rs^* = 0.74 nm

*Stokes radius.
**Equivalent MW of 1200 D as determined by Darnon (2001) with other experiments.
†Mainly peptides and amino acids.

All the solutions were prepared with ultrapure water, and sodium azide was added at 0.2 $g \cdot L^{-1}$ to prevent contamination.

Membrane

UF experiments were carried out using a 15-kD inorganic membrane from Orelis (Carbosep M2). This membrane is composed of a carbon support and a zirconium oxide active top layer. The characteristics of the membrane and its module are given in Table 2. The sieving capacity of the membrane was estimated beforehand, starting from the filtration of size-determined solutes without interactions with the membrane material. Two polyethylene glycol (600 $g \cdot mol^{-1}$ and 6,000 $g \cdot mol^{-1}$) and vitamin B12 (1,355 $g \cdot mol^{-1}$) have been chosen and filtered at various operating conditions (1 to 4 $m \cdot s^{-1}$, 200 to 600 kPa). Figure 2 shows the evolution of the observed transmission rate as a function of molecular weight, at high tangential velocity (4 $m \cdot s^{-1}$) and low transmembrane pressure (200 kPa). Under these conditions, the polarization concentration is reduced to a minimum and the sieving characteristics of the membrane are better underlined. Then, using the film, TIP, and pore approach, the global pore radius was estimated. The results, compiled in Table 3, are in good agreement with those reported by Lucas et al. (1998) for the same membrane.

Experimental apparatus

The experimental setup is shown in Figure 3: a tubular membrane module is fed with constant velocity using a volumetric pump (Wanner Hydra-Cell). The retentate is recycled to the 2L-feed tank, while the permeate is collected or reintroduced into the feed tank. The permeate flow rate is measured in a continuous way, with the balance connected to a computer. The transmembrane pressure is adjusted with a manual valve and measured by a pressure gauge. All experiments are temperature controlled, with the regulation system inside the feed tank.

Table 2. Membrane (carbon support, ZrO_2 layer) and Module Characteristics

Module configuration	Tubular
Membrane dimensions	Internal diameter 6 mm External diameter 10 mm Length 12 cm
Total effective surface	24.5 cm^2
Hydraulic resistance	$4.5 \cdot 10^{12}$ m^{-1}
Surface charge	Isoelectric point : 6.5
MWCO*	15 kD

*Specified by the manufacturer.

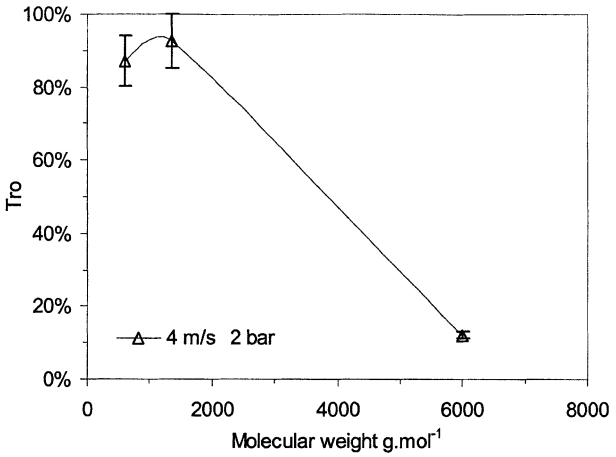

Figure 2. Evolution of Tr_o as a function of molecular weight.

Table 3. Basic Data from Clean Membrane Characterization

Solute	σ	P ($m \cdot s^{-1}$)	rp (nm)	$Ak/\Delta x$ (m^{-1})	Lp ($m \cdot Pa^{-1} \cdot s^{-1}$)
PEG 600	0.227	1.81×10^{-5}	2.6	1.94×10^{5}	1.62×10^{-10}
Vitamin B12	0.138	1.43×10^{-5}	2.9	1.59×10^{5}	1.62×10^{-10}
PEG 6000	0.774	3.78×10^{-7}	2.6	1.86×10^{5}	1.62×10^{-10}

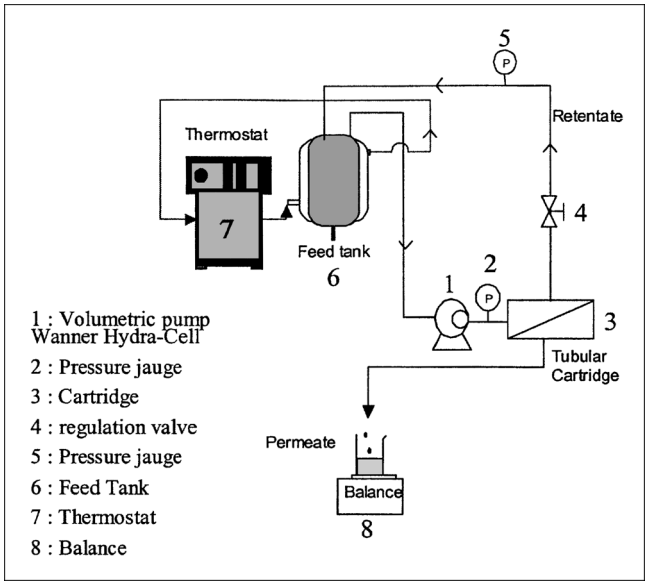

Figure 3. Experimental setup.

Filtration experiments

Cross-flow UF experiments are carried out at constant temperature (20°C), transmembrane pressure (200 KPa), and tangential velocity (2 $m \cdot s^{-1}$). Under these conditions, a turbulent flow settles in the UF module (*Re* numbers higher than 12,000).

Before the experiment, ultrapure water is filtered at constant operating conditions (200 kPa, 2 $m \cdot s^{-1}$, 20°C) so as to calculate the membrane hydraulic resistance, *Rm*, and the pure water permeability, Lp_o. Then, the biological solution is introduced into the pilot apparatus and filtered for 30 min. The permeate is recycled into the feed tank to keep the feed concentration at a fixed level. The steady-state flux is estimated at 30 min; the error on the flux is less than 5%. Similarly, the transmission rate of vitamin B12 is measured with samples (retentate and permeate) collected at 30 min.

At the end of each experiment, the apparatus is rinsed with water and then cleaned with sodium hydroxide (2%, at 80°C, 30 min with 200 kPa) and nitric acid (1%, at 60°C, 30 min with 200 kPa) solutions. The efficiency of the cleaning procedure is checked by pure water filtration: there must be 100% flux recovery.

Analytical procedure

The polyethylene glycol concentrations are estimated using the refractive index measurement of the outlet stream from a size exclusion-HPLC TSK2500PW column.

Vitamin B12 concentration is measured with a spectrophotometer (Unicam 8625) at 361 nm. With an error of 4% on the absorbance measurement, the transmission value is obtained with a precision of 8%.

The protein concentration is estimated using the Bradford colorimetric method. Coomassie reagent (Kit Pierce) is supplied by Pierce. Detection is made at 595 nm.

The total dry extract (DE) is measured by adding 3 mL of samples with 20 g of Fontainbleau sand (Prolabo) at 110°C until a constant weight (24 h is the adequate time) is reached.

The YE concentration is not precisely analyzed, but rather deduced from the DE, B12, and β-lactoglobulin concentrations.

Selectivity analysis

The experimental selectivity of the dynamic membrane for each system is characterized by means of the observed transmission-rate value of the standard molecule vitamin B12, Tr_o^{B12}, defined as the ratio C_p/C_o. Here C_p and C_o are the concentrations ($kg \cdot m^{-3}$), in the permeate and the feed, respectively. Since vitamin B12 is neutral, and has a well-known size, the evolution of its transmission rate is well correlated to the change in the effective sieving capacity of both the clean or fouled membrane: the decreasing value of Tr_o^{B12} indicates a reduction in the effective pore size of the filtering layer, and thus a reduction in the molecular cutoff (MWCO). The membrane is said to be tighter (or more selective).

Filtration of β-Lactoglobulin

A β-lactoglobulin solution containing vitamin B12 as the reference molecule (0.2 $g \cdot L^{-1}$) was filtered. During the filtration, the protein concentration was increased from 1 $g \cdot L^{-1}$ to 10 $g \cdot L^{-1}$, and the vitamin B12 concentration was kept constant. This was accomplished by adding a more concentrated protein solution (40 $g \cdot L^{-1}$) with 0.2 $g \cdot L^{-1}$ of B12. Because the concentration of protein was progressively increased, this experiment is referred to as "continuous." Figure 4 shows the evolution of the vitamin B12 transmission rate and of the permeate flux as a function of the protein concentration.

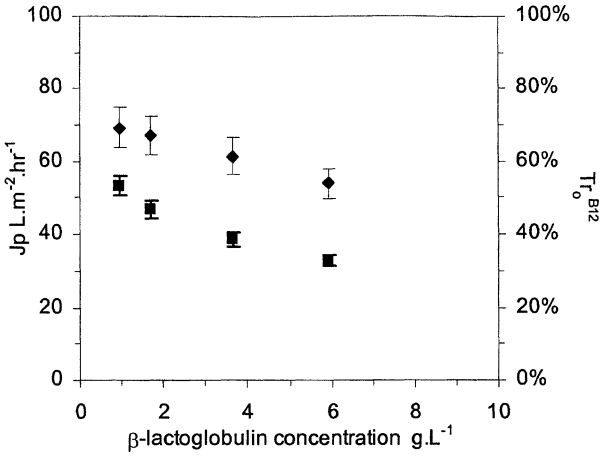

Figure 4. Influence of β-lactoglobulin concentration on *Jp* (■) and Tr_o^{B12} (♦).

The first point to notice is that the membrane sieving characteristics depend on the presence of β-lactoglobulin: the vitamin B12 transmission rate is below 70%, whereas it stands over 85% when B12 is filtered in the absence of protein. These modifications indicate that a dynamic membrane more selective than the initial one settles, whatever the protein concentration.

This figure also reveals that an increasing protein concentration leads to a more resistant (*Jp* is decreasing) and a more selective (Tr_o^{B12} is also decreasing) membrane. This behavior can be easily explained by considering the presence of a growing dynamic membrane, and has already been observed (Matsuyama et al., 1994).

In addition to the concentration, the way the dynamic membrane is formed strongly influences its characteristics. To advance this role, four new experiments were carried out successively, with solutions presenting a constant protein concentration (between 1 and 8 $g \cdot L^{-1}$). In that case, and contrary to what had been done here before, the concentration of the protein was not progressively increased, which is the reason why these experiments are referred to as "discontinuous."

The comparison between these two modes of formation (continuous and discontinuous) is reported in Figure 5. The observed transmission rates of B12 are higher when the concentration is continuously increased during filtration, indicating that the molecular arrangement in the deposit presents a smaller selective dynamic layer. But the mode of formation has no clear influence on the permeate flux.

In the second set of experiments (discontinuous mode) that keep the protein concentration at a fixed level, the reference molecule concentration was increased continuously (from 0.1 $g \cdot L^{-1}$ to 1 $g \cdot L^{-1}$). The experimental points obtained at fixed

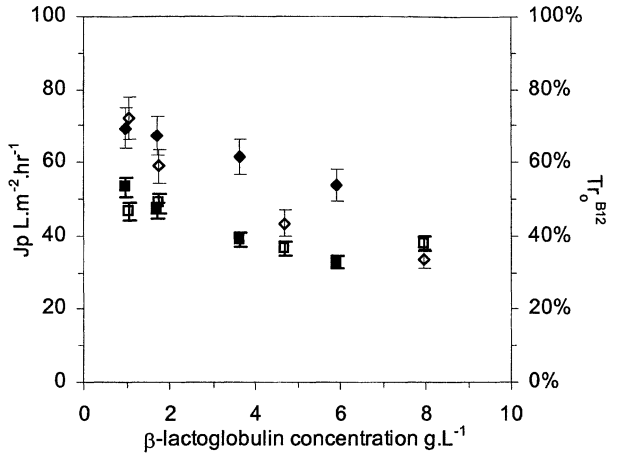

Figure 5. Comparison between the two modes of formation.

Progressive increase of β-lactoglobulin concentration (continuous) (■): Jp; ♦: Tr_o^{B12}; constant β-lactoglobulin concentration (discontinuous) (□): Jp; ◇: Tr_o^{B12}).

protein concentration were analyzed using the film, TIP, and pore approach in order to distinguish the part of the concentration polarization and that of the dynamic layer, and to characterize the fouled membrane. Figure 6 recapitulates the calculation method. The measured data (concentration of β-lactoglobulin and B12, and Jp) are first used to calculate the concentration at the wall, C_m^{β} and C_m^{B12}. Both values are introduced into the estimation of Lp (Eq. 4). Then it becomes possible to estimate rp and $Ak/\Delta x$ using the calculation loop called "determination of rp" in Figure 6. In the first step, rp is initialized. This value is then used to calculate $Ak/\Delta x$ (Eq. 18), P (Eq. 17), and σ (Eq. 16). These last two coefficients are introduced to estimate $Tr_r^{B12calc}$ (Eqs. 6 and 7). Then, $Tr_r^{B12calc}$ is compared with the value obtained directly with the film theory ($Tr^{B12film}$), for each B12 concentration, by means of the sum of the square of the difference between the two Tr_r^{B12}. The loop uses the EXCEL solver to calculate the rp that corresponds to a minimum of this sum.

Table 4. Calculated Characteristics of the Dynamic Membrane (discontinuous mode)

Protein Conc. ($g \cdot L^{-1}$)	σ	P ($m \cdot s^{-1}$)	rp (nm)	$Ak/\Delta x$ (m^{-1})	Lp ($m \cdot Pa^{-1} \cdot s^{-1}$)
1.03	0.47	4.45×10^{-6}	1.84	1.54×10^{5}	6.51×10^{-11}
1.74	0.55	3.41×10^{-6}	1.65	1.71×10^{5}	5.83×10^{-11}
4.71	0.68	1.99×10^{-6}	1.39	2.11×10^{5}	5.12×10^{-11}
7.96	0.72	1.39×10^{-6}	1.31	2.08×10^{5}	4.44×10^{-11}

The calculated σ, P, Lp, rp are reported in Table 4, and plotted as a function of the protein concentration on Figure 7. This figure shows that when C^{β} stands between 1 and 10 $g \cdot L^{-1}$, rp and Lp are well correlated by a logarithmic law, indicating that the more concentrated the protein solution, the more retentive the dynamic membrane. Besides, an increase in concentration also leads to a smaller permeate flux. Since the permeate flux can be expressed as a combination of the osmotic-pressure contribution and the active-layer permeability (Eq. 8), we observe that both are responsible for the smaller flux. On the one hand, the concentration polarization leads to higher C_m when C_o increases; the osmotic pressure is then more important. On the other hand, Lp is lower at high protein concentration, indicating a more resistant layer. It is, however, worth noting that the osmotic pressure is very low as compared to the Lp contribution.

Another set of experiments was performed to account for a dynamic way of forming the layer. In these experiments, the β-lactoglobulin concentration is first increased from 1 $g \cdot L^{-1}$ to a fixed level, and then kept constant while the B12 concentration is increased. The characteristics σ, P, Lp, rp are estimated from this set of data. These values are reported in Table 5. One can observe that the difference between the values of rp obtained by the two modes (previously reported in Table 4) is nearly constant (around to 0.2 nm). Adding to the pore radius, this constant represents the role of the dynamic formation. Figure 8 shows the recalculated values for Jp and Tr_o^{B12} and the experimental ones.

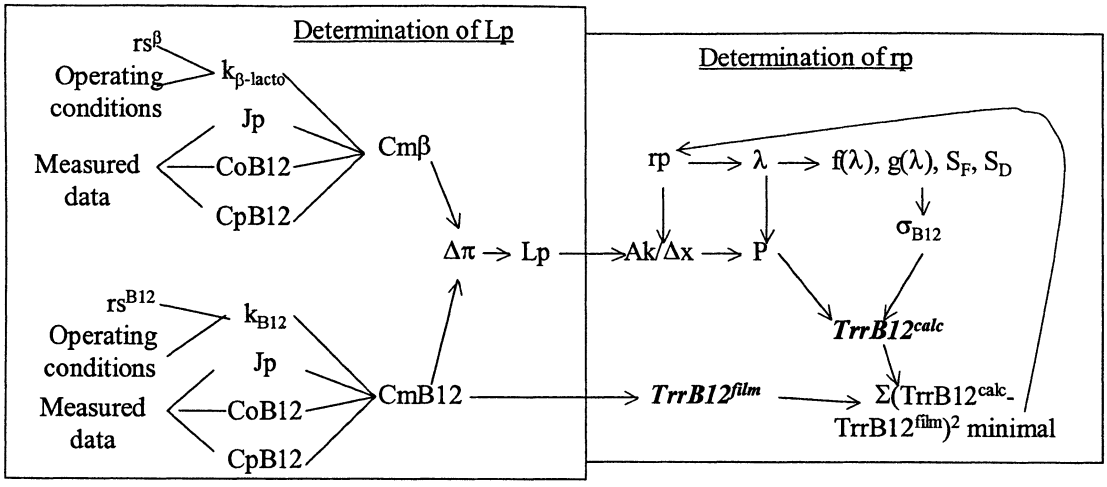

Figure 6. Calculation method for each test at constant β-lactoglobulin concentration and variable B12 concentration.

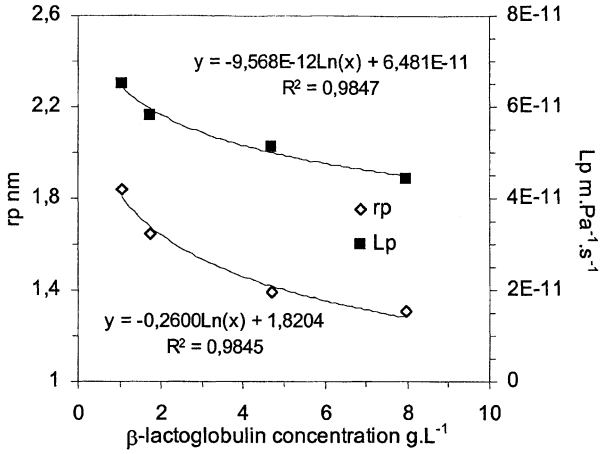

Figure 7. Influence of β-lactoglobulin concentration on the calculated characteristics of the dynamic membrane (noncontinuous formation).

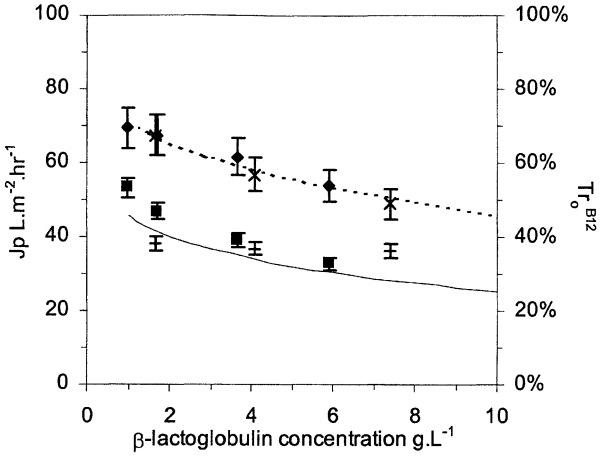

Figure 8. Calculated and experimental evolution of Tr_o^{B12} and Jp as a function of β-lactoglobulin concentration, for β-lactoglobulin alone.

Progressive increase of β-lactoglobulin concentration (continuous) (■): Jp; ♦: Tr_o^{B12}); continuous mode, tests used for the calculation (+ : Jp; × : Tr_o^{B12}).

Filtration of β-Lactoglobulin and Salts

All the previous correlations refer to the filtration of a single-protein solution. Before considering the filtration of a complex mixture, it is worth including in the model the possible effect of the variation of ionic strength.

The influence of ionic strength on the hydraulic permeability and on the sieving characteristics of a protein deposit is quite complex and has been discussed elsewhere. As explained by Opong and Zydney (1991), the solvent properties can affect the behavior of the dynamic layer by either shielding the electrostatic repulsion between adjacent proteins within the deposit, modifying the electroosmotic counterflow, or altering protein conformation. Palecek et al. (1993) observed that the steady-state flow through a protein deposit decreases monotonically with increasing salt concentration. This was proved for five different types of proteins. This trend was explained by assuming a closer packing of the proteins within the deposit due to the increased electrostatic shielding by solutions with a higher salt concentration. Bullon et al. (2000) found the opposite behavior with a stabilized dynamic gelatin layer: in the presence of NaCl, the permeate flux is linearly increasing with the decimal logarithm of the salt concentration. For their part, Rogissart et al. (1991) did not observe any variation in the hydraulic resistance when changing the ionic strength of their filtered solutions (ovalbumine). All these results really emphasized the difficulties encountered in predicting the influence of ionic strength variation on the permeate flux and on the transmission rate of reference solutes. Indeed, the type of the protein has a crucial influence and comes to be added to the pH variation effect. For example, solubility reaches a minimum near the protein isoelectric point.

Table 5. Calculated Characteristics of the Dynamic Membrane (continuous mode)

Protein Conc. ($g \cdot L^{-1}$)	σ	P ($m \cdot s^{-1}$)	rp (nm)	$Ak/\Delta x$ (m^{-1})	Lp ($m \cdot Pa^{-1} \cdot s^{-1}$)
1.03	0.47	4.45×10^{-6}	1.84	1.56×10^{5}	6.51×10^{-11}
1.66	0.47	3.62×10^{-6}	1.83	1.26×10^{5}	5.31×10^{-11}
4.21	0.68	2.81×10^{-6}	1.59	1.63×10^{5}	5.14×10^{-11}
7.42	0.63	2.37×10^{-6}	1.48	1.84×10^{5}	5.07×10^{-11}

To reveal the possible effect of NaCl on the β-lactoglobulin deposit, a set of experiments has been realized by increasing the ionic strength from 0 to 1 M. As seen from Figure 9, the characteristics of the β-lactoglobulin deposit are not clearly linked to the ionic strength. When the ionic strength goes up, the permeate flux and the transmission rate of vitamin B12 do not change significantly. The same conclusions flow from observation of the Jp and Tr_o^{B12} variation vs. protein concentration at 0 and 1 M, respectively (Figure 10). This lack of dependence of Jp and Tr_o^{B12} on the ionic strength cannot be predicted, as it probably depends on the pH value and on the type of electrolyte. In this work, only experiments with NaCl salt at neutral pH have been done. In so far as pH was kept constant in our experiments, and as yeast extract

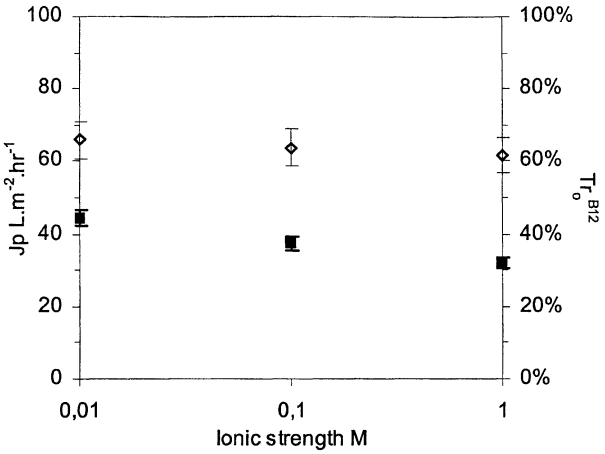

Figure 9. Evolution of Jp (■) and Tr_o^{B12} (◇) as a function of ionic strength.

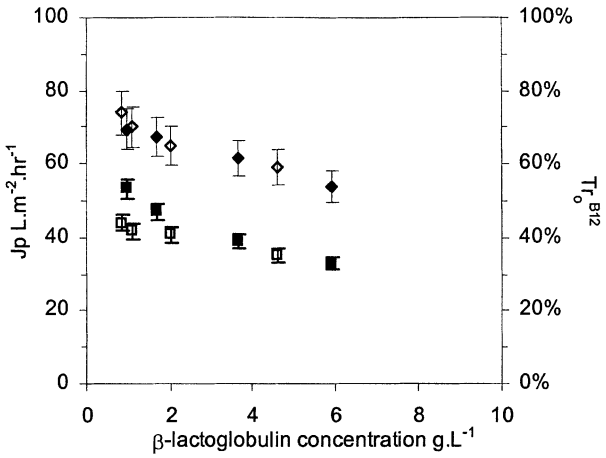

Figure 10. Evolution of *Jp* and Tr_o^{B12} as a function of β-lactoglobulin concentration, at 0 M (■: *Jp*; ♦ Tr_o^{B12}) and 1 M of NaCl (□): *Jp*; ◇: Tr_o^{B12}).

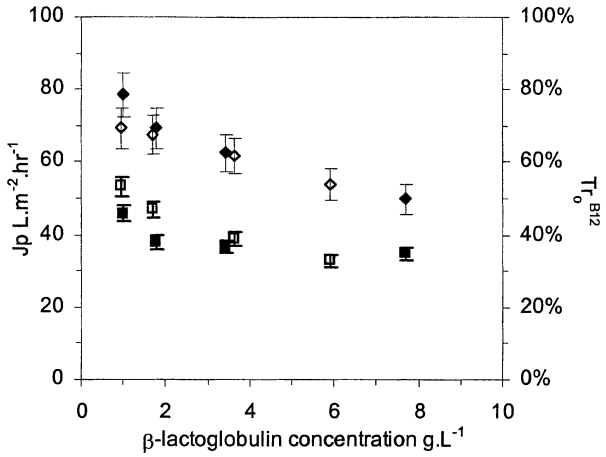

Figure 11. Evolution of *Jp* and Tr_o^{B12} as a function of β-lactoglobulin concentration with 0 (□: *Jp*; ◇: Tr_o^{B12}) and 1 g·L^{-1} of YE (■: *Jp*; ♦: Tr_o^{B12}).

(also added to the solutions) contains mainly monovalent salts, this test (NaCl at neutral pH) was considered as sufficient in the frame of this study. For more information, it is worth recalling that the role of the physicochemical environment, especially of the type of electrolyte used, and the adsorption of calcium or phosphate salts on β-lactoglobulin have been discussed elsewhere (Lucas et al., 1998).

Filtration of β-Lactoglobulin in a Complex Mixture

Yeast extract is a complex mixture containing mainly salts, amino acids, and peptides. As we already said in the Introduction, the complexity prevents any direct calculation of the filtration performance. To extend results obtained with β-lactoglobulin alone, the filtration of a mixture of β-lactoglobulin, YE, and vitamin B12 has been investigated. Each filtration was realized with a constant or an evolutive ratio between YE and β-lactoglobulin concentrations.

Figure 11 allows us to compare the results obtained during the filtration of solutions containing, on the one hand, 1 g·L^{-1} of YE, and on the other hand, no YE. Both *Jp* and Tr_o^{B12} are nearly the same for the two solutions. Yeast extract does not appear to have any influence on the performance. More data are compiled in Figure 12, which plots Tr_o^{B12} and *Jp* when the mixture is filtered at different concentration ratios. No clear influence of the YE concentration on Tr_o^{B12} emerges. At the other hand, it must be noted that the curves obtained at different β-lactoglobulin concentrations are distinct. Regarding flux evolution, an increasing concentration of YE seems to induce lower flux, especially at low β-lactoglobulin concentration.

From all these facts, we can draw the following conclusions:

- Tr_o^{B12}: As no clear effect of YE appear, it can be assumed that the selectivity of the dynamic layer is due to β-lactoglobulin only, and that the dynamic layer is composed mainly of the protein totally rejected by the membrane.
- *Jp*: As for dynamic layer resistance, the role of β-lactoglobulin seems to be dominant. Since no modification of Tr_o^{B12} is observed as a function of YE concentration variation, the small influence of YE on flux can be attributed to the polarization contribution.

Under these elementary assumptions (valuable in the concentration range tested here, from 1 to 10 g·L^{-1}), the permeate flux and the transmission rate of vitatmin B12 for complex mixtures have been simulated using the procedure described on Figure 13 and explained below, assuming no interactions between the solutes in the mixture.

In the first step of the calculation, the correlations on *rp* and *Lp* established with β-lactoglobulin alone are reused to estimate the phenomenological parameters of vitamin B12 as a function of the protein concentration. Then, the YE is added through the osmotic-pressure contribution to estimate the permeate flux. This last determination results from a combination of the TIP equation for flux (Eq. 4) and the film model for the completely rejected protein (Eq. 2). Using this flux and the phenomenological parameters, it becomes possi-

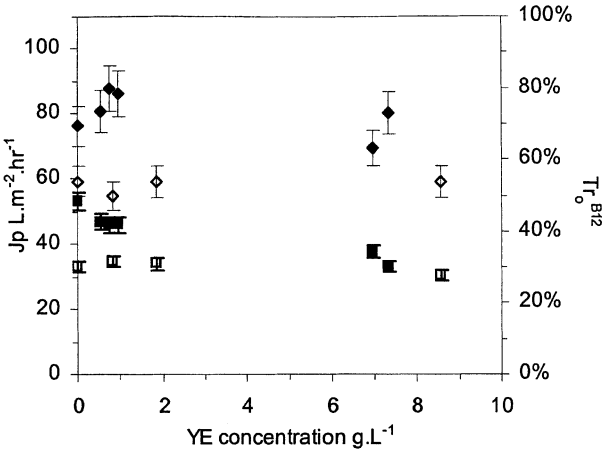

Figure 12. *Jp* and Tr_o^{B12} obtained with different initial concentrations of YE and β-lactoglobulin.

β-lactoglobulin between 0.8 and 1.5 g·L^{-1} (■: *Jp*; ♦: Tr_o^{B12}) and around 10 g·L^{-1} (□: *Jp*; ◇: Tr_o^{B12}).

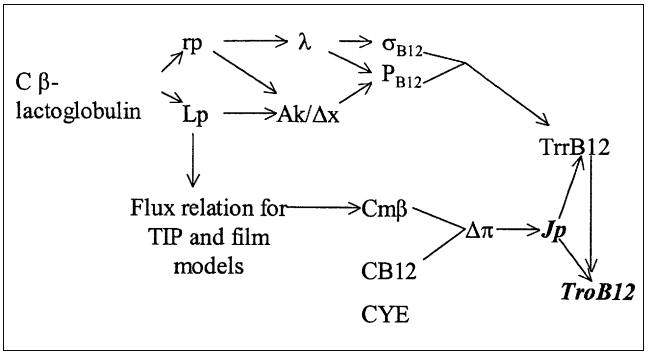

Figure 13. Calculation method to estimate Tr_o^{B12} at different β-lactoglobulin concentration.

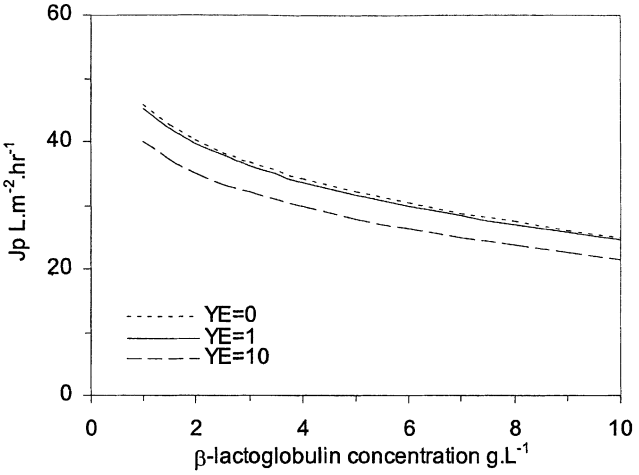

Figure 14. Simulated evolution of *Jp* as a function of β-lactoglobulin concentration (B12 concentration: 0.1 g·L^{-1}).

ble to reach the intrinsic transmission rate of vitamin B12. At least, the film model applied to vitamin B12 gives the observed transmission rate. Simulation results are presented in Figure 14 for various protein and YE concentrations. As expected, we observe that increasing the protein or YE concentration leads to a lower permeate flux. The little influence of

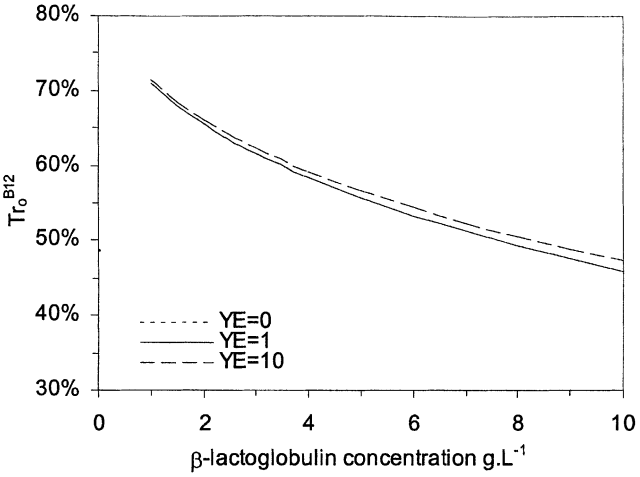

Figure 15. Simulated evolution of Tr_o^{B12} as a function of β-lactoglobulin concentration (B12 concentration: 0.1 g·L^{-1}).

YE concentration on the transmission rate of B12 is due to the permeate flux modifications (Figure 15).

To validate these calculations, Figure 16 compares calculated and experimental data for mixtures. Good agreement is found, indicating that in spite of the evident lack of knowledge of the complex mixture, the simple assumptions used are sufficient to get a correct estimation of performance.

Conclusions

This works shows that:

1. The filtration of a large retained protein (β-lactoglobulin) on a mineral membrane (Carbosep M2) leads to the formation of a dynamic membrane. The role of the protein concentration and of the way this dynamic membrane is formed (continuously or not) is demonstrated. In contrast, the ionic strength (due to NaCl) does not have a significant influence at neutral pH, either on the flux or transmission rate of vitamin B12, the reference molecule.

2. A model of the thermodynamics of irreversible processes and pore theory have been successfully applied to this system. The characteristics *rp* and *Lp* of the dynamic mem-

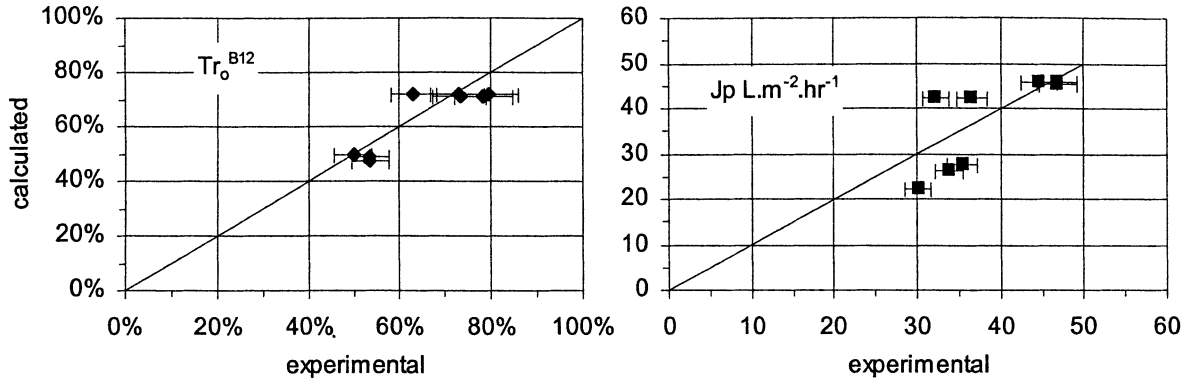

Figure 16. Comparison between experimental and calculated *Jp* and Tr_o^{B12} obtained with mixture (same experimental points as those reported on Figure 12).

brane are correlated with protein concentration through logarithmic laws.

3. When a complex mixture containing yeast extract (YE) and β-lactoglobulin is filtered on the same membrane, the role of the dynamic layer formed by the protein is confirmed. The YE concentration has little effect on the selectivity and on the resistance of the dynamic membrane compared with the influence of the protein concentration.

4. These major assumptions associated with the phenomenological approach lead to a good estimation of results in the case of mixture (flux and transmission rate of vitamin B12). The interest of the new way proposed for simulation, likely extended to complex media, is demonstrated in the case of a solution containing YE, β-lactoglobulin, and vitamin B12; it is possible to recalculate the flux and transmission rate of vitamin B12, a size-calibrated solute present in the mixture.

Literature Cited

Bullon, J., M. P. Belleville, and G. M. Rios, "Preparation of Gelatin Formed-in-Place Membranes: Effect of Working Conditions and Substrates," *J. Memb. Sci.*, **168**, 159 (2000).

Darnon, E., "Intensification des Procédés de Purification de Milieux Biologiques par Intégration de l'Ultrafiltration,"PhD Thesis, Génie des Procédés, Univ. Montpellier II, France (2001).

Lucas, D., M. Rabiller-Baudry, L. Millesime, B. Chaufer, and G. Daufin, "Extraction of Alpha-Lactalbumin from Whey Protein Concentrate with Modified Inorganic Membranes," *J. Memb. Sci.*, **148**, 1 (1998).

Marshall, A. D., P. A. Munro, and G. Trägradh, "The Effect of Protein Fouling in Microfiltration and Ultrafiltration on Permeate Flux, Protein Retention and Selectivity: A Literature Review," *Desalination*, **91**, 65 (1993).

Matsuyama, H., T. Shimomura, and M. Teramoto, "Formation and Characteristics of Dynamic Membrane for Ultrafiltration in Binary Protein System," *J. Memb. Sci.*, **92**, 107 (1994).

Nakao, S. I., and S. Kimura, "Analysis of Solute Rejection in Ultrafiltration," *J. Chem. Eng. Jpn.*, **14**(1), 32 (1981).

Nakao, S. I., "Determination of Pore Size and Pore Size Distribution 3. Filtration Membranes," *J. Memb. Sci.*, **96**, 131 (1994).

Niemi, H., and S. Palosaari, "Calculation of Permeate Flux and Rejection in Simulation of Ultrafiltration and Reverse Osmosis Processes," *J. Memb. Sci.*, **84**, 123 (1993).

Opong, W. S., and A. L. Zydney, "Hydraulic Permeability of Protein Layers Deposited During Ultrafiltration," *J. Colloid Interface Sci.*, **142**(1), 41 (1991).

Palecek, S. P., S. Mochizuki, and A. L. Zydney, "Effect of Ionic Environment on BSA Filtration and the Properties of BSA Deposits," *Desalination*, **90**, 147 (1993).

Palecek, S. P., and A. L. Zydney, "Intermolecular Electrostatic Interactions and Their Effects on Flux and Protein Deposition During Protein Filtration," *Biotechnol. Prog.*, **10**, 207 (1994).

Prabhakar, R., S. DasGupta, and S. De, "Simultaneous Prediction of Flux and Retention for Osmotic Pressure Controlled Turbulent Crossflow Ultrafiltration," *Sep. Purif. Technol.*, **18**, 13 (2000).

Rabiller-Baudry, M., B. Chaufer, P. Aimar, B. Bariou, and D. Lucas, "Application of a Convection-Diffusion-Electrophoretic Migration Model to Ultrafiltration of Lysozyme at Different pH Values and Ionic Strengths," *J. Memb. Sci.*, **179**, 163 (2000).

Rogissard, I., P. Aimar, and W. Gekas. "Etude des Mécanismes de Sélectivité d'une Membrane d'Ultrafiltration," *Récent. Progr. Génie Proc. Cong. Fr. Génie Proc.*, Tech et Doc Lavoisier, Compiègne, p. 37 (1991).

Sarrade, S., G. M. Rios, and M. Carlès, "Dynamic Characterization and Transport Mechanisms of Two Inorganic Membranes for Nanofiltration," *J. Memb. Sci.*, **97**, 155 (1994).

Van den Berg, G. B., I. G. Racz, and C. A. Smolders, "Mass Transfer Coefficients in Cross Flow Ultrafiltration," *J. Memb. Sci.*, **47**, 25 (1989).

Van Reis, R., E. M. Goodrich, C. L. Yson, L. N. Frautschy, R. Whiteley, and A. L. Zydney, "Constant C_{wall} Ultrasonic Process Control," *J. Memb. Sci.*, **130**, 123 (1997).

Verniory, A., R. DuBois, P. Decoodt, J. P. Gassee, and P. P. Lambert, "Measurement of the Permeability of Biological Membranes —Application to the Glomerular Wall," *J. Gen. Physiol.*, **62**, 489 (1973).

Zhao, C., X. Zhou, and Y. Yue, "Determination of Pore Size and Pore Distribution on the Surface of Hollow-Fiber Filtration Membranes," *Desalination*, **129**, 197 (2000).

Manuscript received June 10, 2001, and revision received Jan. 28, 2002.